Low-temperature vortex liquid states induced by quantum fluctuations in the quasi-two-dimensional organic superconductor κ-$(BEDT\text{-}TTF)_2Cu(NCS)_2$

T. Sasaki, T. Fukuda, T. Nishizaki, T. Fujita, N. Yoneyama, and N. Kobayashi
Institute for Materials Research, Tohoku University, Katahira 2-1-1, Sendai 980-8577, Japan

W. Biberacher
Walther-Meissner-Institute, Walther-Meissner Str. 8, D-85748 Garching, Germany
(Received 6 August 2002; published 31 December 2002)

We report the transport properties in the vortex liquid states induced by quantum fluctuations at low temperature in the layered organic superconductor κ-$(BEDT\text{-}TTF)_2Cu(NCS)_2$. A steep drop of the resistivity observed below about 1 K separates the liquid state into two regions. In the low-resistance state at lower temperature, a finite resistivity with weak temperature dependence persists down to 100 mK at least. The finite resistivity in the vortex state at $T \simeq 0$ K indicates the realization of quantum vortex liquid assisted by the strong quantum fluctuations instead of the thermal one. A possible origin for separating these liquid states is a remnant vortex melting line at the original position, which is obscured and suppressed by the quantum fluctuations. A nonlinear behavior of the in-plane resistivity appears at large current density in only the low-resistance state, but not in another vortex liquid state at higher temperature, where the thermal fluctuations are dominant. The transport properties in the low-resistance state are well understood in the vortex slush concept with a short-range order of vortices. Thus the low-resistance state below 1 K is considered to be a novel quantum vortex slush state.

DOI: 10.1103/PhysRevB.66.224513 PACS number(s): 74.70.Kn, 74.60.−w

I. INTRODUCTION

Vortices in the layered superconductors (i.e., high-T_c superconducting oxides, organic superconductors) are affected by strong thermal fluctuations, which have been extensively studied.[1,2] The material parameters of such layered superconductors, implying their short coherence length and large anisotropy of the effective mass, enhance the importance of the fluctuation effects on many supercondicting phenomena such as the thermodynamic and transport properties, and also on the vortex matter dynamics and its phase diagram. Quantum fluctuations in the superconductivity and the vortices are expected to become potentially important at low temperatures in the materials fairly affected by the thermal fluctuations.[3] Indeed the vortex liquid state resulting from the quantum melting at low temperature has been discussed as the quantum vortex liquid (QVL) from several theoretical approaches.[3–9] The favorable material parameters for the experimental observation of quantum fluctuation effects involve a large normal-state resistivity ρ_n, a moderate upper critical field H_{c2} at zero temperature, and a small length scale s for the fluctuations (i.e., short coherence length or short layer separation).

Besides oxides, the BEDT-TTF-molecule-based organic superconductors are also good candidates for the observation of these effects, where BEDT-TTF denotes bis(ethylenedithio)tetrathiafulvalene. The quasi-two-dimensional (Q2D) organic superconductors have relatively large effective normal resistance $R_{eff}=\rho_n/s$ in comparison with the quantum resistance $R_Q=\hbar/e^2$. For example, κ-$(BEDT\text{-}TTF)_2Cu(NCS)_2$, which is investigated in the present study, shows the resistance ratio $Q \equiv R_{eff}/R_Q$ of the order of 10^{-1}, rendering the quantum effects important.[1,5] Further the fairly large Ginzburg number $Gi \equiv (1/2) \times [T_c/H_{c2}^2(0)\varepsilon\xi^3(0)]^2$ of the order of 10^{-1} in κ-$(BEDT\text{-}TTF)_2Cu(NCS)_2$ is in favor of the thermal and also the quantum fluctuations,[1,3] whereas Gi in conventional superconductors is a small number of the order of 10^{-7}, and in oxides, $YBa_2Cu_3O_y$ (YBCO), of the order of 10^{-2}. In the case of the strongly layered oxides, $Bi_2Sr_2CaCu_2O_y$ (BSCCO) possesses $Gi \sim 10^0$.

In addition to the material potential for the quantum fluctuations, it is practically important that a moderate $H_{c2}(0) \simeq 6$–7 T in the magnetic field perpendicular to the Q2D plane can be accessed fully by using standard superconducting magnets. Indeed the QVL state in κ-$(BEDT\text{-}TTF)_2Cu(NCS)_2$ has been found as a reversible magnetization region below H_{c2} even at $T \simeq 0$ K.[10,11]

The transport properties in the QVL state are expected to show some characteristic phenomena such as an insulating behavior.[3,12] The experimental efforts, however, have not been enough to reveal the properties in the QVL state. Most of works have been performed on thin films of conventional superconductors because of meeting the requirement mentioned above.[13–17] The thin films, however, are not so clean that the wide vortex liquid region is not anticipated by the large random pinning force on the vortices. On the other hand, the organic superconductor obtained as a single crystal is so clean that the vortex phase diagram has been discussed in the resemblance with that of BSCCO,[18,19] whereas their T_c's are different by one order of magnitude. Furthermore, the cleanness of the materials enables us to obtain the electronic states in detail by measurements of the magnetic quantum oscillations, de Haas–van Alphen (dHvA) and Shubnikov–de Haas (SdH) effects in the normal[20–22] and also the superconducting[10,23–25] states.

In this paper, we report the transport properties of the title organic superconductor at low temperature, where the QVL state is expected. We are not concerned here with the debatable nature of the superconductivity reported in the κ-type of BEDT-TTF-based organic superconductors, while those are currently discussed on the pairing symmetry and the gap structure[26,27] in connection with the electronic phase diagram in the normal state.[28–30]

II. EXPERIMENT

High-quality single crystals of κ-(BEDT-TTF)$_2$Cu(NCS)$_2$ were grown by an electrochemical oxidation method. The crystals measured have the shape of an elongated hexagonal plate with typical size of $\sim 1.5\times 0.6\times 0.05$ mm^3. The in-plane and out-of-plane resistivities were measured along the b and a^* axes, respectively, by means of a conventional ac or dc four-terminal method. The electrical terminals were made of evaporated gold films, and gold wires (10 μm) were glued onto the films with gold or silver paint. The contact resistance was about 10 Ω for each contact at room temperature, but it became less than 1 Ω at low temperature where the experiments were carried out. The results presented in this paper were obtained on three samples Nos. 1, 2, and 3 from different batches. We found that other three samples measured gave qualitatively similar results which were not presented in this paper. These samples were cooled slowly from room temperature to 4.2 K in 24–48 h in order to avoid the disorder of the terminal ethylene group of the BEDT-TTF molecules. The samples were directly immersed in liquid ^{3}He or the dense ^{3}He gas of the refrigerator which was combined with a 15 T superconducting magnet at the High Magnetic Field Laboratory for Superconducting Materials (HFLSM), IMR, Tohoku University. Sample No. 3 was measured by using the ^{3}He/^{4}He dilution refrigerator with a 14 T superconducting magnet at Walther-Meissner-Institute (WMI). For all measurements reported here, the magnetic field was applied parallel to the a^* axis, i.e., the perpendicular to the Q2D conducting b-c plane.

III. RESULTS AND DISCUSSION

Figure 1 shows the magnetic field dependence of the resistivity (a) ρ_a along a^* axis and (b) ρ_b along b axis of sample No. 1 with dc current I of 10 and 100 μA, respectively. Some curves taken at different temperatures are omitted from the figure because of those overlaps. An anomalous resistance hump is observed in $\rho_a(H)$ curves at temperatures between about 1.5 K and $T_c \simeq 10$ K. The resistivity hump is larger than the isothermal normal resistivity in high magnetic field. In the corresponding temperature–magnetic-field region, the in-plane resistivity ρ_b does not show such an anomaly. This hump anomaly has been reported on only the interlayer resistivity of this material and discussed in several ways.[31–35] But a persuasive explanation has not been presented. Although the purpose of this paper is not on the resistivity hump, it may be a clue for understanding the problem that the phenomena occur in the thermal vortex liquid (TVL) state which is described later.

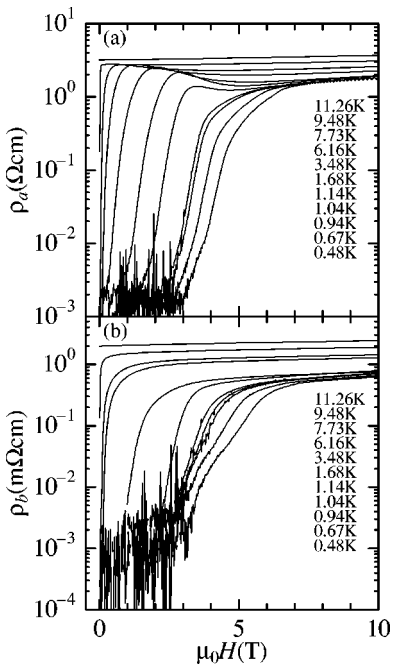

FIG. 1. Magnetic field dependence of the resistivity of κ-(BEDT-TTF)$_2$Cu(NCS)$_2$ in the magnetic field perpendicular to the Q2D plane. (a) The out-of-plane resistivity ρ_a along the a^* axis ($I=10$ μA) and (b) the in-plane resistivity ρ_b along the b axis ($I=100$ μA) are measured in sample No. 1.

The ρ_b curve shows a gradual decrease from the normal resistivity above H_{c2} with decreasing magnetic field. This gradual decrease of the resistivity demonstrates the dissipations due to the flux motion, resulting in the vortex liquid state. Further decreasing the field, the resistivity becomes zero at which the long-range order of vortices starts to grow and the resulting vortex lattice (the vortex solid) is pinned by random pinning-potential-like defects and impurities. Although the solid-liquid transition has been suggested to be a first-order vortex melting one in the low-field region ($\sim$ several ten mT),[36] magnetic measurements in higher fields have shown the transition only as the irreversible field $H_{\rm irr}$.[10,18] In addition the transition at the resistance onset is not so sharp as against the melting transition. It is not clear whether the zero resistivity at the field of tesla order comes in by the first-order melting or the second-order glass-liquid transition.

A steplike structure is found in the ρ_b curves on the way of the gradual transition in the vortex liquid region below 1 K. It means that a low-resistance state appears before achieving zero resistivity. The features of the resistivity and the resulting low-resistance state are found to involve an applied current density dependence.

Figure 2 shows the magnetic field dependence of the in-plane resistivity ρ_b of sample No. 2 in the field perpendicular to the Q2D plane with several dc current density. The applied currents I at 0.51, 0.93, and 1.69 K are 500, 200, 100, 50, 20, 10, and 5 μA and 500, 100, and 10 μA at 4.25 K from the top to bottom curves at each temperature. The current density J corresponding to 500 μA is 1.53 A/cm^2. The transition curves below about 1 K indicate large nonlinear resistance behavior. In the low current density, for example at 0.51 K, a

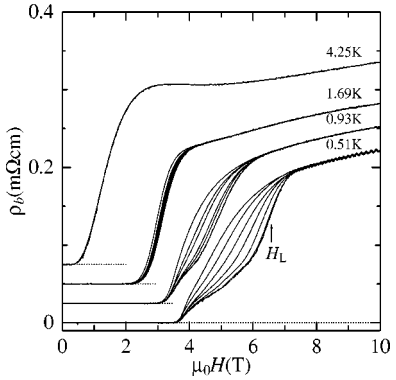

FIG. 2. Magnetic field dependence of the in-plane resistivity ρ_b of sample No. 2 with several current densities in the field perpendicular to the Q2D plane. The applied dc currents are 500, 200, 100, 50, 20, 10, and 5 μA from top to bottom curves at 0.51, 0.93, and 1.69 K and 500, 100, and 10 μA at 4.25 K. Current density J corresponds to the applied current in the ratio of 1.53 A/cm^2 to 500 μA.

steep resistance drop appears at $H_L \simeq 6.5$ T. The low-resistance state following the resistance drop continues down to the field where the resistivity becomes zero. With increasing current density, however, the feature of the resistance drop becomes unclear and the region of the low-resistance state shrinks. No such resistance drop at H_L and, consequently, no low-resistance state are recognized at 1.69 K. It is noted that the observed current density dependence is not caused by the generation of Joule heat in the sample and also at the electrical contacts, because the resistive onset field H_{irr} is not affected by changing the current density, and also the resistive transition curves at 4.25 K, which are measured with the same current density range, coincide with each other.

The resistance drop at H_L and following the low-resistance state are more clearly seen in the temperature dependence of the resistivity at temperatures below 1 K. Figure 3 shows the temperature dependence of the in-plane resistivity ρ_b of sample No. 3. The resistivity measurements were

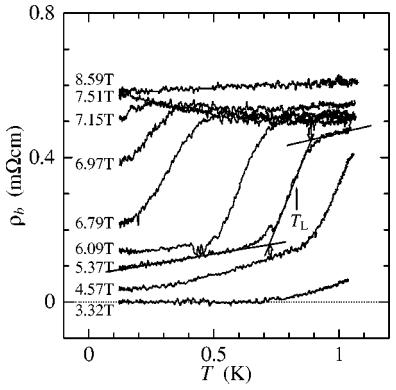

FIG. 3. Temperature dependence of the in-plane resistivity ρ_b in the field perpendicular to the Q2D plane of sample No. 3. The arrows indicate a transition at T_L and the width between the high- and low-resistance states in the vortex liquid state, which are plotted as the bar in the phase diagram of Fig. 4.

performed by ac current (77 Hz) of 20 μA ($j = 0.05$ A/cm^2). The current density in the measurement is almost the same level of that in the two resistivity curves (10 and 20 μA) measured on sample No. 2 in Fig. 2. The resistance drop at T_L corresponding to H_L has a relatively narrow transition width of about 200 mK, which is defined by the intersection points of the linear extrapolation lines to the resistance curve as depicted in Fig. 3. On the other hand, the zero-resistivity transition seems to be gradual as is seen on the curve in 3.32 T and at $T = 0.6$–0.7 K. The gradual transition to zero resistivity may indicate a second-order vortex liquid-glass transition although the transition curve can not be analyzed by the glass scaling law[37,38] because of the insufficient accuracy of the resistance measurements near zero resistivity. The transition curve at T_L shifts almost in parallel to lower temperature with increasing magnetic field, and the feature of the resistance drop can be seen up to nearby $H_{c2}(0) \simeq 7$ T. The low-resistance state following the resistance drop persists down to about 100 mK at least. In addition the temperature dependence of ρ_b in the low-resistance state is relatively weak. Then we expect that the low-resistance state could remain even at $T \simeq 0$ K between ~ 3.5 and ~ 7 T. This finite resistivity is in agreement with the reversible magnetization[10] observed in the QVL state affected strongly by the quantum fluctuations. The quantum melting transition reflected on H_{irr} between the vortex solid and the QVL states at $T \simeq 0$ K has been discussed quantitatively[10] in comparison with the several quantum melting theories.[3–7] Using the material parameters of the present organic superconductor, the quantum melting transition fields have been calculated to be 3.5–4.0 T at $T = 0$ K by different theoretical ways.

It is expected that the quantum fluctuation effect may be seen in the resistance behavior.[3,8] At lower temperature, ρ_b above T_L shows a weak upward curvature, whereas the curve at 8.59 T, where the magnetic field is well above H_{c2}, does not show such a feature. This may indicate an insulating behavior predicted as a strong quantum fluctuation effect at $T \simeq 0$ K and near H_{c2}.[3,12] The resistivity at $T = 0$ K is theoretically expected to take either zero or the normal-state value.[3] It means that either the insulating behavior results in taking the normal-state value or the finite pinning in the real system does in achieving zero resistivity. The intermediate metallic behavior with weak temperature dependence of the resistivity curves from 4.57 T to 7.15 T shows the tendency of neither insulating nor taking zero value down to 0.1 K. This is similar to the observation of the metallic quantum vortex liquid state found in thick amorphous Mo_xSi_{1-x} films at $T \simeq 0$ K.[17] In order to confirm this point in the present organic superconductor, further experiments at lower temperatures and in finely tuned magnetic fields are required.

The experimentally obtained H_L, T_L, and the low-resistance state with nonlinear behavior apparently show that the vortex liquid state of this material is separated into two kinds of the vortex liquid; one is the thermally fluctuated vortex liquid at high temperature and another the nonlinear low-resistance vortex slush[39] like state where the quantum vortex liquid may be realized by the strong quantum fluctua-

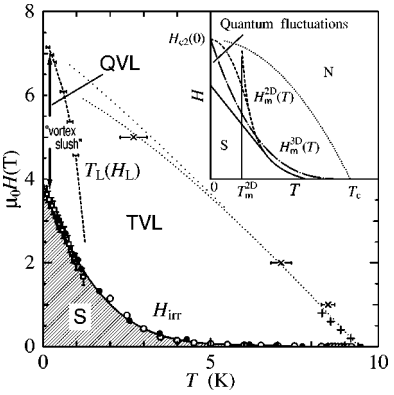

FIG. 4. Vortex phase diagram of κ-(BEDT-TTF)$_2$Cu(NCS)$_2$ in the magnetic field perpendicular to the Q2D plane. QVL and TVL are the quantum and thermal vortex liquid states. N and S denote the normal and the vortex solid states. The lower dotted curve shows the ordinary H_{c2} including the effect of fluctuations. The curve is determined by the specific heat (Ref. 40) (pluses) and the magnetization (Ref. 41) (crosses) measurements. The expected mean-field H_{c2} line is plotted by another dotted curve (upper side). H_{irr} indicates the irreversible magnetic field obtained by the magnetization (Ref. 18) (open circles), the magnetic torque (Ref. 10) (open squares), and the resistivity measurements in the present study (solid circles). The dashed line T_L (H_L) separates the vortex liquid state into two regions: the thermal vortex liquid (TVL) state with high resistivity at high temperature and the vortex-slush-like low-resistance state at low temperature. The inset shows a schematic phase diagram of the layered superconductors. For details see the text.

tion instead of the thermal one at low temperature.

Figure 4 shows the phase diagram of the vortex system in the magnetic field perpendicular to the Q2D plane of κ-(BEDT-TTF)$_2$Cu(NCS)$_2$. In the main panel the hatched low-T, low-H region is the vortex solid state (S), which is characterized by the zero resistance and the irreversible magnetization. The squares and circles are the irreversible field H_{irr} determined by the magnetic torque[10] and superconducting quantum interference device[18] (SQUID) measurements, respectively. The solid circles are determined as the onset magnetic field of ρ_a in Fig. 1(a). The resistivity level of 2×10^{-3} Ω cm is used for the criterion of the onset. The resistive onset magnetic fields for ρ_b agree with those for ρ_a by extrapolating the ρ_b data to the same criterion level (6×10^{-4} mΩ cm) which is 10^{-3} times smaller than the normal-state value. The pluses and crosses are the ordinary upper critical field H_{c2} obtained by the specific heat[40] and the magnetization.[41] The lower dotted curve of the ordinary H_{c2} on the pluses and crosses is expected to be lowered from the mean field H_{c2} (the upper dotted curve) due to fluctuations.[3] Above the H_{irr} line in the TVL region, the vortices do not have any long-range order, resulting in the vortex liquid state. Most of the liquid state (TVL) above several hundred mT is considered to be formed by melting or decoupling from the pinned vortex pancakes[18,19] in the S state. The transition is mainly assisted by thermal fluctuations. In the very-low-magnetic-field region below the dimensional crossover at several ten mT, the Abrikosov vortex line lattice exists.[19,42] On the low-magnetic-field phases which are not included in Fig. 4, refer to previous reports.[18,19]

The dashed line (T_L and H_L) separates the vortex liquid state into two regions mentioned above. One is the TVL state at higher T, and the other the nonlinear low-resistance state at lower T. This low-resistance state persists down to at least 100 mK in $H_{irr}<H<H_{c2}$ at $T\simeq0$ K. The transport properties in the low-resistance state below H_L resemble those observed in the vortex slush phase which has been found between the vortex liquid and glass phases of the high-T_c oxide superconductors having an intermediate range of disorder.[39,43] The vortex slush phase has the short-range order of the vortices,[39,44,45] which is characterized by the nonlinear resistivity.[39,43,46,47] The transition between the vortex liquid and slush phases appears as a steep resistance drop but not to zero and also a small magnetization jump.[43,47] This transition is thought to be an incomplete first-order phase transition at the same transition field and temperature of the original one hidden by the disorder effect. In addition the second-order vortex glass transition line appears between the vortex slush and glass phases.

Let us discuss the correspondence between the nonlinear low-resistance state found in this material and the vortex slush phase with a short-range order of vortices. The inset of Fig. 4 shows schematic phase diagram of the layered superconductors.[1,48] In the case of the three-dimensional (3D) materials, e.g., YBCO, the melting line (the dotted chain) points to $H_{c2}(0)$ because of less effect of the fluctuations. In contrast to the 3D system, the melting line (the dashed line) of the 2D materials, e.g., BSCCO and the present organic superconductor, increases rapidly near the 2D melting temperature T_m^{2D}, which is independent of magnetic field at the Berezinskii-Kosterlitz-Thouless (BKT) type dislocation-mediated melting transition,[49] $kT_m^{2D}=d\varepsilon_0/8\sqrt{3}\pi$, where $\varepsilon_0=(\Phi_0/4\pi\lambda)^2$, k is Boltzmann's constant, d the layer spacing, Φ_0 the flux quantum, and λ the in-plane penetration depth. The magnetic-field-independent T_m^{2D} is expected at 1.5–2.5 K in the present organic superconductor with $d\simeq15.2$ Å (Ref. 50) and the in-plane $\lambda\simeq5000$–7000 Å.[19,41,42,51] In the real material the 2D melting line is expected to get away from T_m^{2D} and turn toward $H_{c2}(0)$ in high magnetic field.

The T_L (H_L) line observed in this material seems to coincide with the above-mentioned melting line T_m^{2D}, which corresponds to the dislocation-mediated melting line,[5] following the dashed line in the inset. In practice, however, the quantum fluctuations and finite amount of disorders in the real system push the actual solid-liquid line (H_{irr} and the solid line in the inset) down to lower magnetic fields, for example in the present material, down to about 4 T even at $T\simeq0$ K. Thus the H_L line is considered to have the similar nature of the remnant solid-liquid line at the original position where the short-range order of vortices starts to grow, but it does not develop to the long-range order with zero resistivity. In addition the resulting vortex liquid is considered to be QVL at low temperatures. The low-resistance state is, therefore, concluded to be a novel *quantum vortex slush* state.

The H_L line seems to exceed the ordinary H_{c2} line at $T\simeq0$ K. This looks to be inconsistent with the above scenario

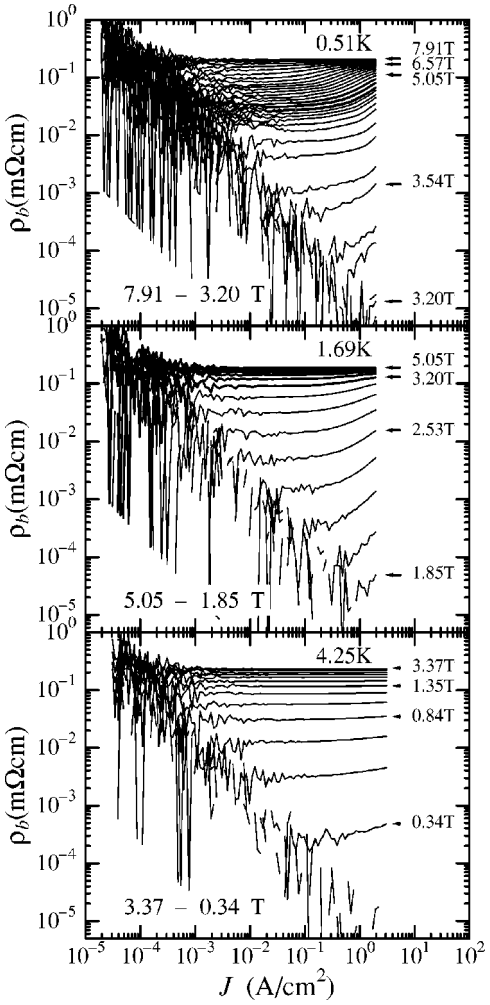

FIG. 5. Current density dependence of the in-plane resistivity ρ_b of sample No. 2 in magnetic fields perpendicular to the Q2D plane. The curves are measured in intervals of about 0.17 T from 7.91 (top curve) to 3.20 T (bottom), from 5.05 to 1.85 T, and from 3.37 to 0.34 T at 0.51, 1.69, and 4.25 K, respectively.

of $H_{c2}=H_L$ at $T=0$ K. The Lindemann-type approach for the vortex melting theory leads the melting point always below H_{c2} at $T=0$ K.[5] Recently Ishida and Ikeda[52] have argued the melting transition near $T=0$ K by their quantum Ginzburg-Landau approach. They have suggested that the melting transition is possible to occur above the ordinary H_{c2} at $T\simeq 0$ K in the clean system and the quantum-dissipated three-dimensional case. It must be theoretically important to investigate the relation among H_L, H_{irr}, the ordinary H_{c2}, and the mean field H_{c2} at $T\simeq 0$ K.

Turning now to investigate the vortex-slush-like state characterized by the nonlinear transport behavior, Fig. 5 shows the current density dependence of the in-plane resistivity ρ_b of sample No. 2 in magnetic fields perpendicular to the Q2D plane at 0.51, 1.69, and 4.25 K. The current-density (J)—resistivity (ρ_b) characteristic curves are measured in intervals of about 0.17 T from 7.91 (top curve) to 3.20 T (bottom), from 5.05 to 1.85 T, and from 3.37 to 0.34 T at 0.51, 1.69, and 4.25 K, respectively. At 0.51 K (top panel), two regions of the constant ρ_b as a function of J, that is, the linear E-J behavior, in low current density are separated around $H_L\simeq 6.5$ T. One is the linear resistivity in high magnetic fields near H_{c2}, and the other linear resistivity appears around 6 T. In between these two regions, the steep drop of the linear resistivity at low J is found as spreading the spacing between curves. Then, below about 6 T, the linear resistivity stops dropping as fast. Only at lower magnetic fields approaching H_{irr} does the downward curvature of the ρ_b-J curve set in and the linear part of the resistivity vanish within the present experimental accuracy. This indicates that the low-resistance state below H_L has nonzero linear resistivity at low J. At high J, the low-resistance state becomes unclear and shows the nonlinear E-J behavior, which has been seen in Fig. 2. This nonlinear behavior at high J can be also explained in the vortex slush scheme. The vortex slush resistivity at low J increases to the vortex liquid resistivity at high J by moving the vortex lattice domains with short-range order due to the Magnus force. The domains pass over the pinning sites. For larger J, the vortex domains move like as vortex liquid, and hence a higher resistivity is induced. Actually, as is seen in the top panel at 0.51 K, the smaller J required for moving the domain, namely, where the ρ_b-J curve starts to deviate from the constant, is necessary with coming close to the magnetic field H_L (or T_L). At a high temperature of 1.69 K (middle panel), just outside of the vortex-slush-like region, the linear resistivity at low J shows a continuous drop and then changes to the nonlinear one with downward curvature due to the pinning near H_{irr}. Only the linear resistivity is observed within the applied J in this experiment at 4.25 K (bottom panel).

As just described above, the observed E-J response in the low-resistance state is well explained by the concept of the vortex slush which has been proposed experimentally by Worthington *et al.*[39] and theoretically discussed by Ikeda,[44] although both studies have focused attention on the oxide high-T_c superconductors. These studies have been examined also by Monte Carlo simulations.[45] While most of the characteristic features observed in this study are very well understood in the vortex slush concept, some points remain unclear. First, the linear resistivity in low J in the vortex slush has been expected to come from thermal excitation, and then the exponential decrease of ρ with T has been predicted.[39] This exponential temperature dependence contradicts the observed weak temperature dependence as shown in Fig. 3. Second, the vortex slush state in the oxide high-T_c superconductors has been found only in the sample with the intermediate range of the disorders which have been controlled by the proton irradiation[39] and the oxygen concentration.[43,47] The organic superconductor in the present study is generally considered to be a clean system but with a finite weak disorder. These must closely connect to the relation among the origin (thermal or quantum) of the excitations (fluctuations), those strength of fluctuations at the temperature, and a degree of the finite pinning strength. A theoretical approach for the quantum effect on the vortices is necessary for further understanding of the present phenomena.

Finally we would like to mention the H_L (T_L) transition from the different aspects of the magnetic quantum oscillations. The dHvA oscillations have been observed not only in

the normal state but also the vortex state below H_{c2}.[10,23,24] The amplitude of the oscillations in the vortex state has been reduced by an additional damping effect with respect to the normal-state damping.[53] The dHvA effect in the vortex liquid state of the present organic superconductor has been understood in the thermal fluctuation approach.[24,53] Recently SdH oscillations in the vortex liquid state have been reported.[25] The SdH oscillations have been able to be observed down to 5 T at 0.5 K, where the resistivity becomes about 30% of the normal-state value. The additional damping of the SdH amplitude has appeared below about 7 T as well as the dHvA oscillations. In addition the novel stronger damping has been found only in the SdH effect below about 6 T at 0.5 K. The latter damping suppresses the SdH oscillation amplitude rapidly as compared to the former damping below H_{c2}. In view of the vortex phase diagram in the present study, the magnetic field where the latter damping starts to appear corresponds to the H_L line. The amplitude of the dHvA oscillations in the vortex state has been calculated to be perturbed by the phase coherence of the vortices.[53] In the vortex slush state the coherence may vary with applied current. The current dependence of the phase coherence in the vortex slush state may explain why the amplitude of SdH oscillations is smaller than that of the dHvA one below H_L. It must be, however, necessary for further consideration of the different ways of the amplitude damping of both the dHvA and SdH effects in the vortex liquid (QVL or TVL) and the vortex slush states in addition to the normal and the Abrikosov vortex lattice states.

IV. SUMMARY

We have reported the nonlinear low-resistance state in the vortex liquid state of the quasi-two-dimensional organic superconductor κ-$(BEDT\text{-}TTF)_2Cu(NCS)_2$. The low-resistance state appears below about 1 K, which is separated from the thermal vortex liquid state by the characteristic drop of the in-plane resistivity at T_L and H_L. A possible origin of the drop of the resistivity is a hidden freezing transition which is obscured by strong quantum fluctuations.

The low-resistance state at lower temperature persists down to $T \simeq 0$ K in $H_{irr} < H < H_{c2}$. The finite resistivity remaining at $T \simeq 0$ K and the reversible magnetization demonstrate that the quantum vortex liquid state is realized there. The drop of resistivity at T_L and H_L comes from the linear resistivity at low J in the low-resistance state. By applying a high J the linear resistivity changes to the higher vortex liquid resistivity with nonlinear response. These transport phenomena are well understood in the vortex slush concept, which is characterized by a short-range order of the vortices. As a result, the low-resistance state is concluded to be a novel *quantum vortex slush* state. In order to confirm the quantum vortex slush in the low-resistance state, it is important to investigate the thermodynamic properties at H_L and how the the H_L and H_{irr} lines are connected.

ACKNOWLEDGMENTS

The authors thank R. Ikeda and T. Maniv for stimulating discussions. One of the authors (T.S.) acknowledges the support of a dilution refrigerator experiment at WMI by K. Neumaier and W. Hehn. A part of this work was performed at HFLSM, IMR, Tohoku University. This work was partly supported by a Grant-in-Aid for Scientific Research from the Ministry of Education, Science, Sports, and Culture of Japan.

[1] G. Blatter, M.V. Feigel'man, V.B. Geshkenbein, A.I. Larkin, and V.M. Vinokur, Rev. Mod. Phys. **66**, 1125 (1994).
[2] T. Nishizaki and N. Kobayashi, Supercond. Sci. Technol. **13**, 1 (2000).
[3] R. Ikeda, Int. J. Mod. Phys. B **10**, 601 (1996).
[4] G. Blatter and B. Ivlev, Phys. Rev. Lett. **70**, 2621 (1993).
[5] G. Blatter, B. Ivlev, Y. Kagan, M. Theunissen, Y. Volokitin, and P. Kes, Phys. Rev. B **50**, 13 013 (1994).
[6] E.M. Chudnovsky, Phys. Rev. B **51**, 15 351 (1995).
[7] A. Rozhkov and D. Stroud, Phys. Rev. B **54**, R12 697 (1996).
[8] T. Onogi and S. Doniach, Solid State Commun. **98**, 1 (1996).
[9] A. Krämer and S. Doniach, Phys. Rev. Lett. **81**, 3523 (1998).
[10] T. Sasaki, W. Biberacher, K. Neumaier, W. Hehn, K. Andres, and T. Fukase, Phys. Rev. B **57**, 10 889 (1998).
[11] M.M. Mola, S. Hill, J.S. Brooks, and J.S. Qualls, Phys. Rev. Lett. **86**, 2130 (2001).
[12] R. Ikeda, J. Phys. Soc. Jpn. **65**, 33 (1996).
[13] D. Ephron, A. Yazdani, A. Kapitulnik, and M.R. Beasley, Phys. Rev. Lett. **76**, 1529 (1996).
[14] P.H. Kes, M.H. Theunissen, and B. Becher, Physica C **282-287**, 331 (1997).
[15] N. Marković, A.M. Mack, G. Martinez-Arizala, C. Christiansen, and A.M. Goldman, Phys. Rev. Lett. **81**, 701 (1998).
[16] J.A. Chervenak and J.M. Valles, Jr., Phys. Rev. B **61**, R9245 (2000).
[17] S. Okuma, Y. Imamoto, and M. Morita, Phys. Rev. Lett. **86**, 3136 (2001).
[18] T. Nishizaki, T. Sasaki, T. Fukase, and N. Kobayashi, Phys. Rev. B **54**, R3760 (1996).
[19] S.L. Lee, F.L. Pratt, S.J. Blundell, C.M. Aegerter, P.A. Pattenden, K.H. Chow, E.M. Forgan, T. Sasaki, W. Hayes, and H. Keller, Phys. Rev. Lett. **79**, 1563 (1997).
[20] K. Oshima, T. Mori, H. Inokuchi, H. Urayama, H. Yamochi, and G. Saito, Phys. Rev. B **38**, 938 (1988).
[21] T. Sasaki, H. Sato, and N. Toyota, Solid State Commun. **76**, 507 (1990).
[22] N. Harrison, J. Caulfield, J. Singleton, P.H.P. Reinders, F. Herlach, W. Hayes, M. Kurmoo, and P. Day, J. Phys.: Condens. Matter **8**, 5415 (1996).
[23] P.J. van der Wel, J. Caulfield, R. Corcoran, P. Day, S.M. Hayden, W. Hayes, M. Kurmoo, P. Meeson, J. Singleton, and M. Springford, Physica C **235-240**, 2453 (1994).

[24] N.J. Clayton, H. Ito, S.M. Hayden, P.J. Meeson, M. Springford, and G. Saito, Phys. Rev. B **65**, 064515 (2002).
[25] T. Sasaki, T. Fukuda, N. Yoneyama, and N. Kobayashi, cond-mat/0203228 (unpublished).
[26] K. Izawa, H. Yamaguchi, T. Sasaki, and Y. Matsuda, Phys. Rev. Lett. **88**, 027002 (2002), and references therein.
[27] J. Müller, M. Lang, R. Helfrich, F. Steglich, and T. Sasaki, Phys. Rev. B **65**, 140509(R) (2002), and references therein.
[28] K. Kanoda, Hyperfine Interact. **104**, 235 (1997).
[29] T. Sasaki, N. Yoneyama, A. Matsuyama, and N. Kobayashi, Phys. Rev. B **65**, 060505 (2002), and references therein.
[30] J. Müller, M. Lang, F. Steglich, J.A. Schlueter, A.M. Kini, and T. Sasaki, Phys. Rev. B **65**, 144521 (2002), and references therein.
[31] F.L. Pratt, J. Caulfield, L. Cowey, J. Singleton, M. Doporto, W. Hayes, J.A.A.J. Perenboom, M. Kurmoo, and P. Day, Synth. Met. **55-57**, 2289 (1993).
[32] H. Ito, T. Ishiguro, T. Komatsu, G. Saito, and H. Anzai, Physica B **201**, 470 (1994).
[33] S. Friemel, C. Pasquier, and D. Jerome, Physica C **292**, 273 (1997).
[34] F. Zuo, J.A. Schlueter, M.E. Kelly, and J.M. Williams, Phys. Rev. B **54**, 11 973 (1996).
[35] M.V. Kartsovnik, G.Yu. Logvenov, K. Maki, and N.D. Kushch, Synth. Met. **103**, 1827 (1999).
[36] M. Inada, T. Sasaki, T. Nishizaki, N. Kobayashi, S. Yamada, and T. Fukase, J. Low Temp. Phys. **117**, 1423 (1999).
[37] M.P.A. Fisher, Phys. Rev. Lett. **62**, 1415 (1989).
[38] D.S. Fisher, M.P.A. Fisher, and D.A. Huse, Phys. Rev. B **43**, 130 (1991).
[39] T.K. Worthington, M.P.A. Fisher, D.A. Huse, J. Toner, A.D. Marwick, T. Zabel, C.A. Feild, and F. Holtzberg, Phys. Rev. B **46**, 11 854 (1992).
[40] J.E. Graebner, R.C. Haddon, S.V. Chichester, and S.H. Glarum, Phys. Rev. B **41**, 4808 (1990).
[41] M. Lang, F. Steglich, N. Toyota, and T. Sasaki, Phys. Rev. B **49**, 15 227 (1994).
[42] L.Ya. Vinnikov, T.L. Barkov, M.V. Kartsovnik, and N.D. Kushch, Phys. Rev. B **61**, 14 358 (2000).
[43] T. Nishizaki, K. Shibata, T. Sasaki, and N. Kobayashi, Physica C **341-348**, 957 (2000).
[44] R. Ikeda, J. Phys. Soc. Jpn. **70**, 219 (2001).
[45] Y. Nonomura and X. Hu, Phys. Rev. Lett. **86**, 5140 (2001).
[46] H.H. Wen, S.L. Li, G.H. Chen, and X.S. Ling, Phys. Rev. B **64**, 054507 (2001).
[47] K. Shibata, T. Nishizaki, T. Sasaki, and N. Kobayashi, Phys. Rev. B (to be published).
[48] M. Tinkham, *Introduction to Superconductivity*, 2nd ed. (McGraw-Hill, New York, 1996).
[49] B.A. Huberman and S. Doniach, Phys. Rev. Lett. **43**, 950 (1979).
[50] N. Toyota, Y. Watanabe, and T. Sasaki, Synth. Met. **55-57**, 2536 (1993).
[51] M. Lang, N. Toyota, T. Sasaki, and H. Sato, Phys. Rev. Lett. **69**, 1443 (1992).
[52] H. Ishida and R. Ikeda, J. Phys. Soc. Jpn. **71**, 254 (2002).
[53] T. Maniv, V. Zhuravlev, I. Vagner, and P. Wyder, Rev. Mod. Phys. **73**, 867 (2001).